Variable-range hopping conductivity in $La_{1-x}Ca_xMnO_3$

2001 J. Phys.: Condens. Matter 13 1233

(http://iopscience.iop.org/0953-8984/13/6/304)

INSTITUTE OF PHYSICS PUBLISHING JOURNAL OF PHYSICS: CONDENSED MATTER

J. Phys.: Condens. Matter **13** (2001) 1233–1246 www.iop.org/Journals/cm PII: S0953-8984(01)16234-X

Variable-range hopping conductivity in $La_{1-x}Ca_xMnO_3$

R Laiho[1,3], **K G Lisunov**[2], **E Lähderanta**[1], **V N Stamov**[2] **and V S Zakhvalinskii**[2]

[1] Wihuri Physical Laboratory, Department of Physics, University of Turku, FIN-20014 Turku, Finland
[2] Institute of Applied Physics, Academiei Street 5, MD-2028 Kishinev, Moldova

E-mail: erlah@utu.fi (R Laiho)

Received 9 August 2000, in final form 13 November 2000

Abstract

In ceramic $La_{1-x}Ca_xMnO_3$ samples with $0 \leqslant x \leqslant 0.15$ and the concentration of holes $c = 0.18$–0.22 between $T = 77$ and 340 K the resistivity, ρ, is shown to have an activated character both above and below the ferromagnetic Curie temperature, T_C. The temperature dependence of the local activation energy, $E_{loc}\ (T) = \mathrm{d}\ln\rho(T)/\mathrm{d}(kT)^{-1}$ gives evidence for a variable-range hopping conductivity over states of the Coulomb gap. The width of the gap $\Delta \approx 0.24$ eV, the effective dielectric permeability $\kappa \approx 3.6$ and the carrier localization radius $\xi \approx 5.1$ Å in the paramagnetic phase are determined. The value of ξ suggests hopping of small lattice polarons at $T > T_C$. With decreasing temperature two successive transitions, at temperatures T_C' and T_C'', associated with divergence of the correlation length, are observed in the vicinity of T_C. They can be interpreted in terms of critical increase (as T approaches T_C' from higher temperatures) and decrease (when T shifts from T_C'' towards lower temperatures) of the radius of magnetic polarons, generated by a small fraction of the lattice polarons as $T \to T_C$. The difference between T_C and the temperature of the first divergence of ξ, $T_C' < T_C$, gives evidence of percolative character of the FM–PM transition.

1. Introduction

$La_{1-x}Ca_xMnO_3$ (LCMO for short) is a mixed-valence perovskite compound obtained by substitution of La for Ca in the antiferromagnetic (AFM) insulator $LaMnO_3$. Insertion of a divalent alkaline element into La sites greatly modifies the electronic and magnetic properties of the parent alloy by creating holes in the singlet Mn state by change of some Mn^{3+} ions to Mn^{4+} [1]. Other sources of holes are cation lattice vacancies [2] or deviations from the exact oxygen stoichiometry [3]. Competition between the AFM Mn^{3+}–Mn^{3+} superexchange interaction and the ferromagnetic (FM) double-exchange Mn^{3+}–Mn^{4+} interaction yields different magnetic

[3] Author to whom any correspondence should be addressed. Telephone: 358-2-3335943; fax: 358-2-2319836.

phases in LCMO at different intervals of the temperature T, the composition x and the hole concentration, c [4, 5]. Another reason for persistent interest in LCMO over recent years is the very large drop of the resistivity, ρ, in an external magnetic field, known as 'colossal magnetoresistance' (CMR) [6]. CMR attains its maximum value near the temperature of the transition from the paramagnetic (PM) to the FM state, T_C, for the compound with $x \approx 0.3$. For x between $\sim$0.2 and 0.5 the FM transition coincides with the metal–insulator transition (MIT). At $x < 0.2$ LCMO remains insulating both above and below T_C [7]. Extensive investigations have shown that the nature of CMR and the variety of magnetic properties of LCMO and related compounds cannot be understood without considering the significance of lattice or magnetic polarons [7–9]. Distortion of the local environment around Mn^{3+} ions associated with the Jahn–Teller effect and formation of lattice polarons has been established by x-ray absorption measurements on LCMO with $0.2 < x < 0.5$ over a wide range of T both above and below T_C [10]. A liquid-like spatial distribution of small magnetic polarons has been observed in a Mössbauer study of the compounds with $x = 0.05$ and 0.08 [11]. From powder neutron diffraction measurements on $La_{1-x}Sr_xMnO_3$ with $x = 0.2$ and 0.4 it has been concluded that the lattice and magnetic polarons represent basically the same excitation [12].

Small-polaron hopping has been used to interpret different transport properties (resistivity, Hall effect and thermoelectric power) in the insulating phase of LCMO and related compounds [13–16]. It has also been argued that coherent motion of small polarons may contribute to the resistivity of the metallic phase in LCMO [17]. However, information about the nature of the resistivity in compounds where MIT does not take place at T_C, namely when x is small, corresponding to the insulating phase over the whole temperature range, is still lacking. In the previously cited papers the temperature dependence of the resistivity of CMR compounds has been explained on the basis of an activated process following a simple Arrhenius law. On the other hand, in references [18–23] clear deviations from the Arrhenius law both in bulk samples and in thin films of different CMR materials have been observed. The Mott mechanism [24] of variable-range hopping (VRH) has been suggested to interpret conductivity in these papers. However, little attention has been paid to other possible reasons for the VRH conductivity. Here we present investigations of the resistivity in the insulating phase of LCMO, demonstrating clearly that the VRH conductivity of LCMO is determined by the Shklovskii–Efros mechanism [25] which sets in when the Coulomb interaction between the charge carriers is important. It is also shown that the analysis of the hopping conductivity in different temperature regions gives important information, which is closely related to details of the magnetic state of the system.

2. Experimental results

The LCMO samples with $x = 0$, 0.05 and 0.15 (denoted below as #1, #2 and #3) were synthesized with the conventional ceramic technique (see e.g. [5]) by mixing stoichiometric amounts of La_2O_3, $CaCO_3$ and MnO_2 and heating in air with intermediate grindings. X-ray diffraction measurements showed that all samples were of single phase, having the undistorted cubic structure (space group *Pm3m*). From dc magnetization measurements the values of c and T_C collected in table 1 were obtained [26]. The deviation of c from the corresponding value of x is connected with formation of vacancies in the metallic sublattice during preparation of the sample.

Measurements of the resistivity function $\rho(T)$ between $T = 77$ and 340 K with the standard four-probe technique yielded the same result for increasing and decreasing values of T. As shown in figure 1 the resistivity of the samples #1 and #2 has an activated semiconductor-like character over the whole temperature range. Near T_C a clear inflection is observed in the $\rho(T)$ curves. For sample #3 this inflection has the shape of a shallow maximum with a small

Table 1. The composition (x), the relative (c) [18] and absolute (n_h) concentrations of holes, the Curie temperature (T_C) [18], the characteristic VRH temperature (T_0'), the onset temperature of VRH (T_v), the width of the Coulomb gap (Δ'), the dielectric permeability (κ') and the localization radius (ξ') in the stable regime of LCMO.

Sample No	x	c	n_h (10^{20} cm^{-3})	T_C (K)	T_0' (10^4 K)	T_v (K)	Δ' (eV)	κ'	ξ' (Å)
#1	0.00	0.21	4.45	172	2.73	275	0.235	3.7	4.6
#2	0.05	0.18	3.82	173	2.46	317	0.240	3.5	5.4
#3	0.15	0.22	4.66	190	2.43	320	0.240	3.7	5.2

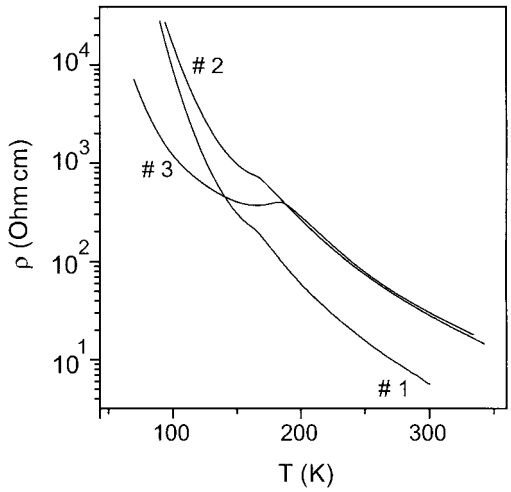

Figure 1. The experimental temperature dependence of the resistivity for samples #1, #2 and #3.

interval of metal-like behaviour just below T_C. Generally, the shapes of the $\rho(T)$ curves and the resistivity values resemble those for $La_{1-x}A_xMnO_3$ with A = Ca [15, 27, 28], Ba or Sr [7] at low x in the FM insulating part of the magnetic phase diagram.

The temperature dependence of the susceptibility χ was measured with a SQUID magnetometer after cooling the sample from 310 to 5 K in zero ($B < 0.1$ G) field (ZFC) or in a field of 2 G (FC). As is evident from figure 2, the PM-to-FM transition appears in all of the samples with the values of T_C equal to those collected in table 1. Additionally, the onset of a strong magnetic irreversibility indicated by deviation of $\chi_{ZFC}(T)$ from $\chi_{FC}(T)$ is observed at a temperature slightly below T_C. Such irreversibility is a signature of a spin-glass (SG) phase, which has been confirmed by investigations of long-time relaxation of the thermo-remanent magnetization [29] and the frequency dependence of the ac susceptibility [30] for the same specimens.

3. Analysis of the results

For crystalline semiconductors with a well-defined energy gap the activated character of the conductivity may be determined by thermal activation of electrons from the valence band to the conduction band (intrinsic conductivity) or from the impurity levels (impurity conduction). Another determinant is hopping of localized electrons from a state below the Fermi level to a state above it inside the impurity band (hopping conductivity) [25]. The hopping mechanism is

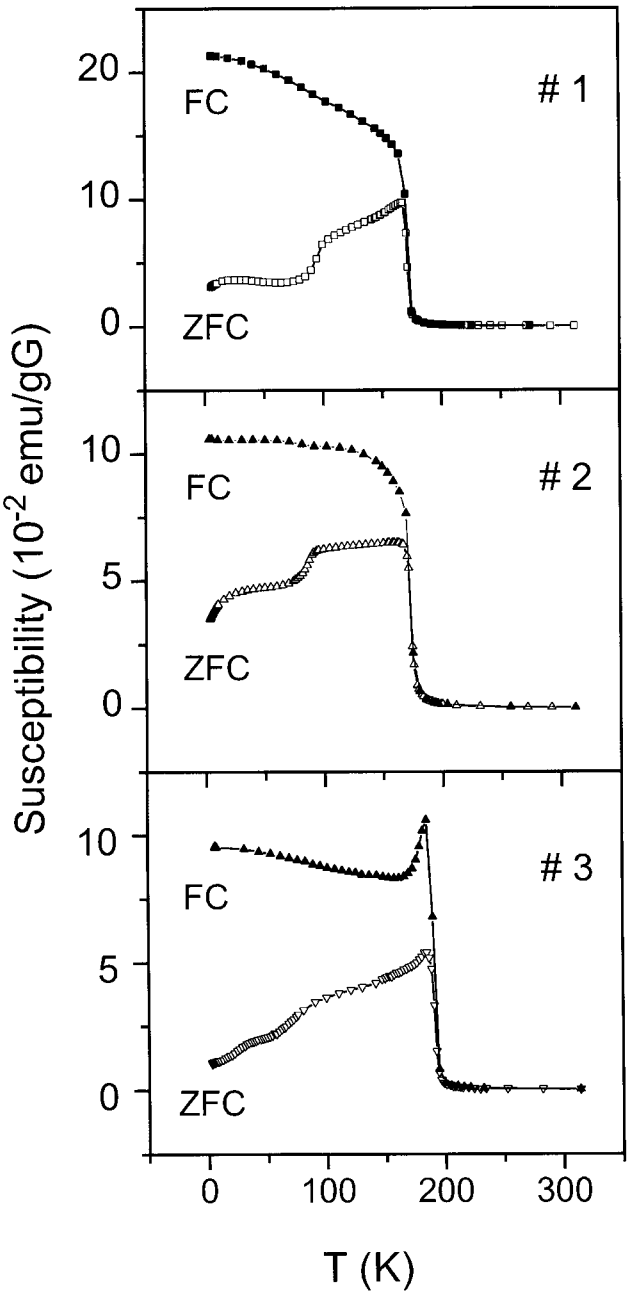

Figure 2. The temperature dependence of χ_{ZFC} and χ_{FC} for samples #1, #2 and #3.

often responsible for the conductivity of non-crystalline materials [24] when the carrier density of localized states (DOS) is a continuous function of the energy. Thermally activated hopping transport may also be realized when the carriers are lattice or magnetic polarons [24]. Because in LCMO the intrinsic conductivity has been observed at very high temperatures ∼1000 K [27], it is not considered below.

The impurity conduction and the hopping conductivity over the nearest sites (NSH) obey a similar Arrhenius-like law:

$$\rho(T) = \rho_0 \exp(E_a/kT) \tag{1}$$

where the prefactor ρ_0 is only a weak function of temperature and the activation energy E_a does not depend on T. In some cases it is energetically favourable for a localized carrier to hop to a site beyond the nearest-neighbour centres. Then the average hopping length exceeds the average distance between the sites, and the VRH conductivity sets in [24, 25]. In this regime E_a is not constant but depends on T. The aforementioned cases include those where the DOS is constant within some interval of energy around the Fermi level μ (the Mott-VRH regime [24]) or has a parabolic gap with the width Δ due to the Coulomb interaction between the localized carriers (the Shklovskii–Efros or SE-VRH regime [25]). In all of these cases the activation energy can be written in a universal form

$$E_a(T) = kT\left(\frac{T_0}{T}\right)^p \tag{2}$$

where T_0 is a constant and $p = 1$, 1/4 or 1/2 for the NSH conductivity, the Mott-VRH and the SE-VRH conductivity, respectively.

In the SE-VRH regime the prefactor in equation (1) $\rho_0 \sim T^{1/2}$ [31], while in the Mott regime $\rho_0 \sim T^s$ where a variety of values of the exponent $s = -1/4, -3/4$ [25] or $-3/8$ [31] have been proposed depending on details of the applied model. On the other hand, in all of these cases the temperature dependence of the prefactor ρ_0 in the Mott regime is much weaker than the exponential one and can be neglected while maintaining sufficient accuracy. Therefore, to identify the type of VRH conductivity a usual practice is to plot $\ln[T^{-1/2}\rho(T)]$ versus $T^{-1/2}$ or $\ln[\rho(T)]$ versus $T^{-1/4}$ to obtain a straight line. However, as is evident from figures 3(a) and 3(b), below T_C the two plots represent straight lines of the same quality. In such a situation evaluation of the local activation energy [25]

$$E_{loc}(T) = \frac{\mathrm{d}\ln\rho(T)}{\mathrm{d}(1/kT)} \tag{3}$$

is an effective method for identification of the type of hopping. As follows from equations (1)–(3), neglecting the weak temperature dependence of ρ_0, the slope of the linear dependence of $\ln[E_{loc}(T)/kT]$ on $\ln T$ gives the value of $-p$.

As can be seen from figure 4, the plots of $\ln[E_{loc}(T)/kT]$ versus $\ln T$ for samples #1 and #2 have sharp minima at $T_m = 163$ and 165 K, respectively. For #3 a steep decrease is observed as T approaches the temperature $T_m = 164$ K from above or $T_m^* = 183$ K from below. Due to a metallic behaviour, evident also from figure 1, E_{loc} does not exist within the gap between T_m and T_m^*. At $T_m < T < T_v$ a constant slope with p close to 1/2 (the dashed lines in figure 4) satisfies the SE-VRH requirement. On a larger scale between $T \sim 180$ and 340 K the plots of $\ln[E_{loc}(T)/kT]$ versus $\ln T$ are shown in figure 5. The values of p in figure 5, obtained from a least-squares fit with the error of $\sim$10% , provide clear evidence for the SE-VRH regime in all of the samples investigated. The values of T_v are collected in table 1. For convenience we distinguish the 'stable regime' with a constant slope of the plots of $\ln[E_{loc}(T)/kT]$ versus $\ln T$, and the 'critical regime' with a steep variation of E_{loc}. The latter is realized when T approaches T_m (or T_m^*) from both sides, while the former exists only above T_m. Below T_m or T_m^* the plots of $\ln[E_{loc}(T)/kT]$ versus $\ln T$ cannot be characterized by a constant slope with sufficient accuracy within any significant temperature interval. This suggests a crossover between the stable and the critical regimes when T is decreased below the region of pure critical behaviour. The proximity of T_m to T_C shown by the dotted line in figure 3 is also noticeable.

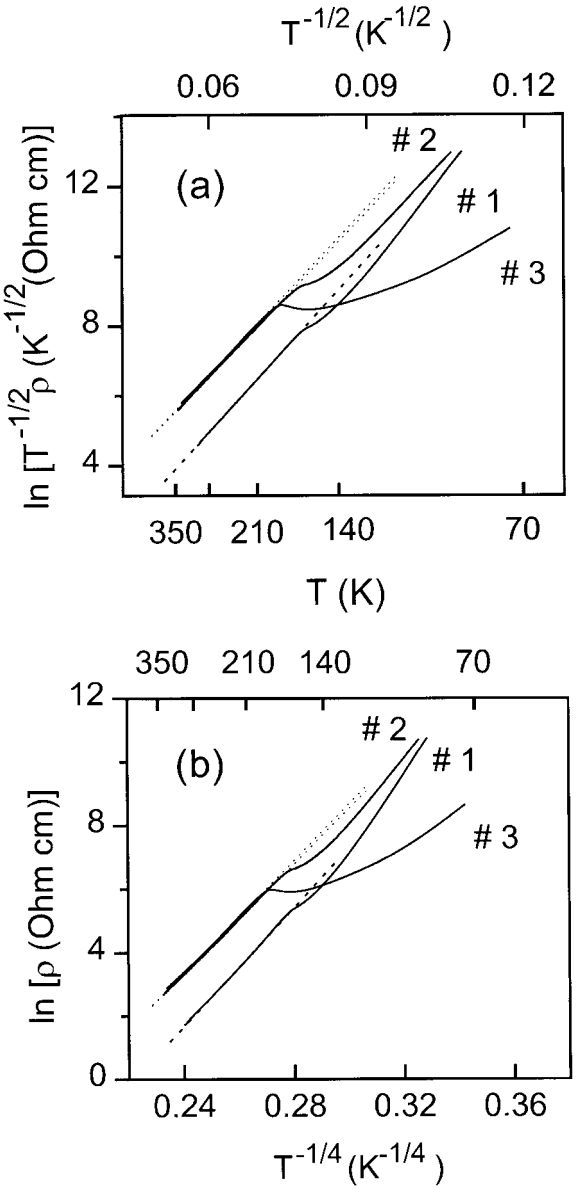

Figure 3. The resistivity versus $T^{-1/2}$ (a) and $T^{-1/4}$ (b) for samples #1, #2 and #3. The dotted lines represent the fits to a linear function.

Assuming the SE-VRH mechanism we analyse our data separately in the intervals of $T > T_m$ (where all characteristic parameters are marked with a single prime, e.g. T_0', ξ' etc) and $T < T_m$ (using the double prime, T_0'', ξ'' etc) and exclude the interval between T_m and T_m^*. According to the SE model [25] the VRH characteristic temperature T_0 and the width of the gap Δ can be written as

$$T_0 = \frac{\beta e^2}{k\kappa\xi} \qquad \Delta = 2\frac{e^3 g_0^{1/2}}{\kappa^{3/2}} \tag{4}$$

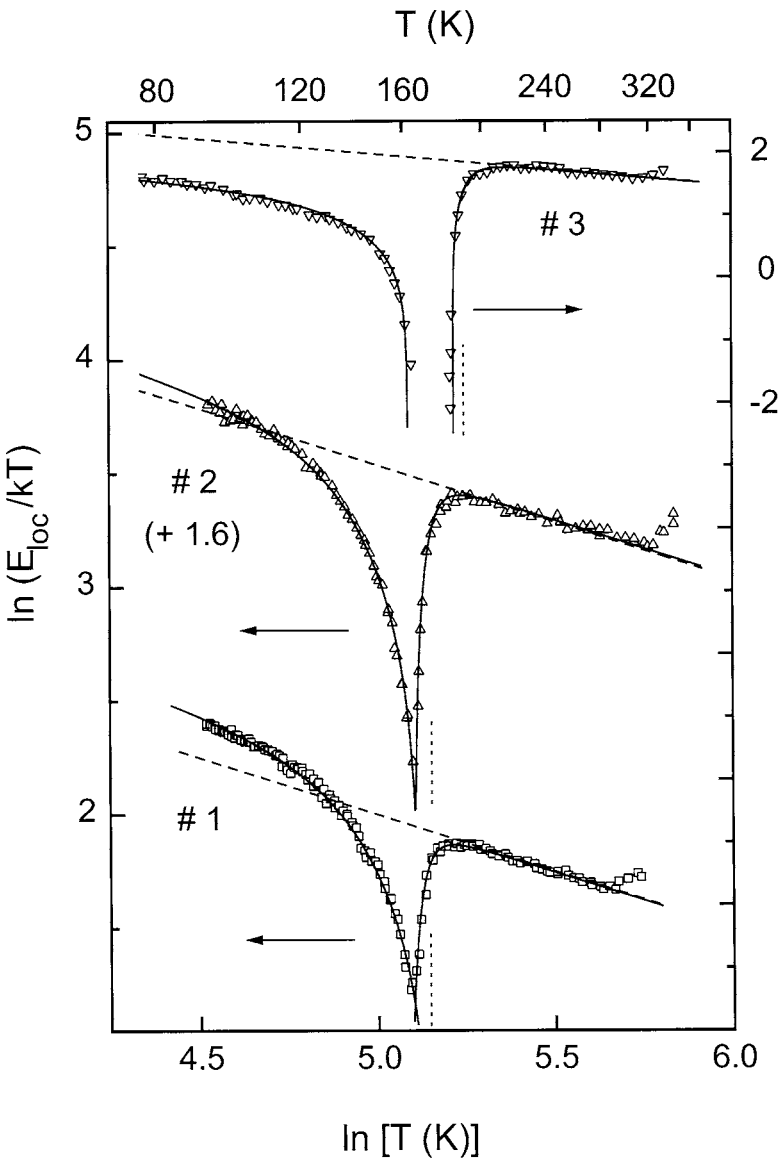

Figure 4. Local activation energy versus temperature for samples #1, #2 (shifted by 1.6 units along the y-axis) and #3. The dashed lines correspond to the slope $-1/2$. The solid lines are calculated as described in the text. The vertical dotted lines mark the values of T_C.

where ξ is the correlation length or the localization radius of a hopping carrier, κ is the dielectric permeability, $\beta = 2.8$, g_0 is the value of the DOS outside the gap and N_s is the concentration of hopping sites taken equal to the hole concentration n_h (see table 1). A transition to the SE-VRH conductivity takes place when $E_a(T)$ becomes equal to Δ. This condition and equation (2) allow Δ to be expressed in terms of the experimentally observable parameters T_0 and T_v (the temperature of the onset of the VRH) as

$$\Delta = k\sqrt{T_0 T_v}. \tag{5}$$

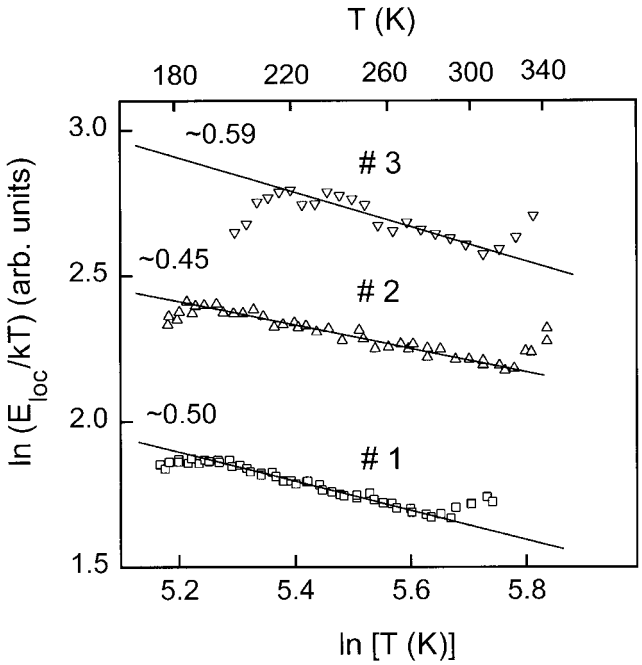

Figure 5. Local activation energy versus temperature for samples #1, #2 and #3 between 180 and 340 K in an enlarged scale. The solid lines are the linear fits; the corresponding values of p are shown.

The values of T_0' were found from the slopes of the linear dependence of $\ln(T^{-1/2}\rho)$ versus $T^{-1/2}$ (see figure 3 (a)) in the stable regime between T_m and T_v (see table 1). Then the values of Δ' were evaluated using equation (5) (they are listed in table 1 also). As shown by magnetization measurements, the carriers are localized in LCMO within an interval of width $W \approx 1.9$ eV [26]. Therefore, taking into account that $\Delta' \ll W$ and approximating the DOS with a function of rectangular shape, the values of the DOS outside the gap evaluated from the equation $g_0 \approx n_h/W$ are found to be 2.34×10^{20}, 2.01×10^{20} and 2.45×10^{20} eV^{-1} cm^{-3} for the samples #1, #2 and #3, respectively. Then κ' and ξ' are obtained from equations (4). The values of ξ', κ' and Δ', collected in table 1, do not show any systematic dependence on x. According to the SE model, Δ is approximately equal to the energy of the Coulomb interaction between the carriers. This energy can be found from the equation

$$U' \approx e^2/\kappa' R_s \tag{6}$$

where $R_s = 2(4\pi N_s/3)^{1/3}$ is the average distance between the hopping sites giving $U' \approx 0.24$ eV in agreement with the values of Δ' found above. Hence, the application of the SE model provides a consistent description of VRH in the stable regime at $T > T_m$.

To analyse $E_{loc}(T)$ in the critical regime we suppose that the critical behaviour of the correlation length obeys the scaling law

$$\xi(T) = \xi_0 \tau^{-\nu}. \tag{7}$$

Here ξ_0 is independent of T and equal to ξ in the stable regime, ν is the critical exponent of the correlation length, $\tau' = (1 - T_C'/T)^{-\nu'}$ at $T > T_m$, $\tau'' = (1 - T/T_C'')^{-\nu''}$ at $T < T_m$, and T_C' and T_C'' are the critical temperatures. From equations (1)–(3) we obtain with $p = 1/2$

$$\ln \frac{E_{loc}(T)}{kT^{1/2}} = -\ln 2 + C + \frac{\nu}{2} \ln \tau \tag{8}$$

where $C = (1/2)\ln T_0$. The parameters T_C' and T_C'' (see table 2) were inserted to obtain a linear dependence of the left-hand side of equation (8) on $\ln\tau$ as $T \to T_m \pm 0$ (see figure 6). Then these plots were fitted with a linear law (the solid lines in figure 6) to find the values of C', ν' and C'', ν''. They are collected in table 2. The critical exponents are found to be sample and temperature independent and close to unity. The critical temperatures exhibit different behaviour: T_C' increases while T_C'' decreases when x is increased. Additionally, the ratio $T_C'/T_C = 0.95 \pm 0.02$ is nearly constant. The values of C'' decrease systematically with x, while C' is practically independent of x. The above analysis shows that the correlation length of the carriers in the critical regime can be well described with the scaling law (7) on

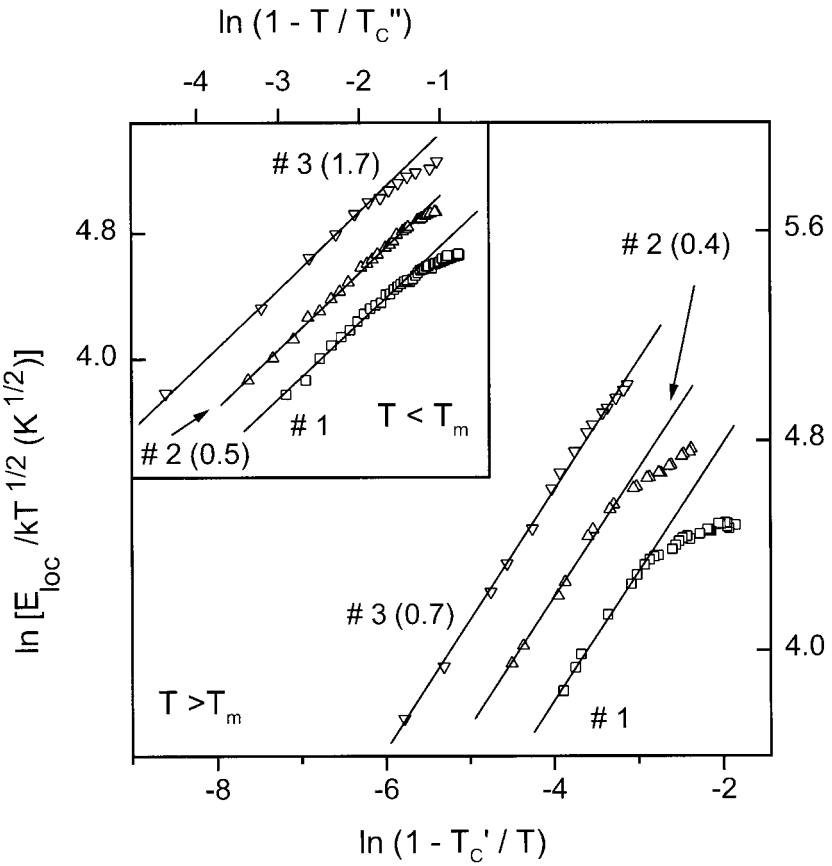

Figure 6. Critical behaviour of the local activation energy versus temperature for samples #1, #2 and #3 at $T > T_m$ and $T < T_m$ (inset). The solid lines are the fits to linear functions. In parenthesis we show the shifts of the corresponding curves along the y-axis.

Table 2. The values of the fitting parameters in the critical regime.

Sample No	T_C' (K)	ν'	C'	$(1/2)\ln T_0'$	ζ' (10^{-4})	T_C''	ν''	C''
#1	159	0.98	6.46	5.11	3.0	172	0.97	5.89
#2	165	0.98	6.45	5.06	2.4	165	0.98	5.72
#3	185	0.99	6.49	5.02	2.0	162	0.99	4.92

both sides of T_m. However, in general the description of $E_{loc}(T)$ at $T > T_m$ is inconsistent. In table 2 we show also the values of $(1/2)\ln T_0'$ (the argument of the logarithm is in K) evaluated with T_0' obtained previously in the stable regime (table 1). The large difference between the values of C' and $(1/2)\ln T_0'$ gives evidence that the critical and the stable regimes cannot be described simultaneously assuming equation (7) with ξ_0' equal to the correlation length (ξ') which has been found previously in the stable regime. In other words, the correlation length should exhibit a discontinuity in such a description when the transition from the stable to the critical regime takes place, whereas no discontinuity is observed in the temperature dependence of E_{loc} at $T > T_m$.

This contradiction does not appear if we suppose two types of hopping carrier with the concentrations n_1 and n_2 satisfying the condition of $\eta \equiv n_2/n_1 \approx n_2/n_h \ll 1$ and with the temperature-independent correlation lengths $\xi_1 = \xi$ equal to that in the stable regime, and $\xi_2(T) = \xi_{02}\tau^{-\nu}$ satisfying a scaling law similar to equation (7) with ξ_{02} independent of T. The mean correlation volume per carrier is defined by $V = (n_1V_1 + n_2V_2)/n_h$ where $V_j = 4\pi\xi_j^3/3$ $(j = 1, 2)$. Then the mean correlation length satisfies the equation

$$\xi(T) = \xi_1(1 + \zeta\tau^{-3\nu})^{1/3} \tag{9}$$

where $\zeta \equiv \eta(\xi_{02}/\xi_1)^3 \ll 1$ if ξ_1 and ξ_{02} are comparable. As follows from equation (9), due to the smallness of ζ in the stable regime we have $\xi(T) \approx \xi_1$ which does not depend on T. In the critical regime $\xi(T) \approx \xi_1\zeta^{1/3}\tau^{-\nu}$ because of the unlimited growth of τ as T approaches T_C' or T_C''. Therefore, the results obtained above for both regimes remain the same but the value of C is connected to T_0 by the equation $C = D - (1/6)\ln\zeta$ where $D = (1/2)\ln T_0$. This gives $\zeta = \exp(3\ln T_0 - 6C)$. Using the values of C' from table 2, we obtain those of ζ' which are collected in the same table. It is seen that the condition of $\zeta' \ll 1$ is well satisfied. Using equations (1)–(3) and (9), we obtain the equation

$$\ln\frac{E_{loc}(T)}{kT} = -\ln 2 + D - \frac{1}{2}\ln T - \frac{1}{6}\ln(1 + \zeta\tau^{-3\nu}) \tag{10}$$

which should be valid both in the stable and in the critical regime. We fit the dependence of $E_{loc}(T)$ from equation (10), taking $\nu = 1$ on both sides of T_m, and find a complete agreement with the experimental data (see figure 4). The values of T_C', D' and ζ' $(T < T_m)$ and T_C'', D'' and ζ'' $(T > T_m)$ are collected in table 3. As follows from comparison of the data in tables 2 and 3, the values of T_C' and T_C'' obtained by the fitting of $E_{loc}(T)$ in the critical regime alone and over the whole temperature range are very close, and those of ζ' are similar. From both fits we conclude that ζ' is approximately independent of x.

Table 3. The values of the fitting parameters over the whole temperature interval.

Sample No	T_C' (K)	D'	ζ' (10^{-4})	T_C'' (K)	D''	ζ''
#1	162	5.19	2.4	173	5.44	0.06
#2	165	5.14	2.7	167	5.25	0.05
#3	185	5.16	4.2	162	4.50	0.07

Next, the values of D' are found close to $(1/2)\ln T_0'$, thus removing the aforementioned contradiction of discontinuity of the correlation length at $T > T_m$. A good agreement between the experimental and the calculated data at $T < T_m$ supports the conclusion that in this temperature interval the stable regime is not reached down to the lowest temperature used in the measurements. The values of ζ'' are $\ll 1$ but much higher than ζ'. They do not exhibit a systematic dependence on x, with the result that the ratio ξ_{02}''/ξ_1'' is nearly constant.

Additionally, the relation $C'' - D'' = -(1/6)\ln\zeta''$ is satisfied with a high accuracy, indicating the absence of a discontinuity of the correlation length also at $T < T_m$. The parameters C'' and D'' are found to be linear functions of $\ln(1 - x/x_t)$ with $x_t \approx 0.175$ and the angular coefficient is very close to 0.5 (see figure 7). Taking into account the first of equations (4) and the definition of C'' and D'', this means that both lengths, ξ_1'' and ξ_{02}'', as well as ξ'' as a whole, exhibit the scaling behaviour $\xi'' \sim (1 - x/x_t)^{-\nu}$ with $\nu \approx 1$.

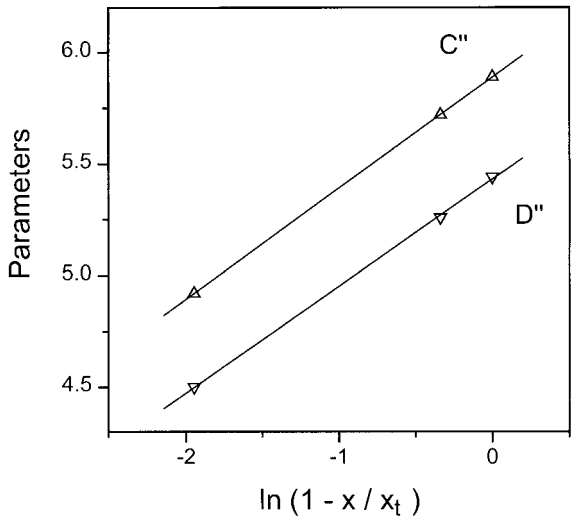

Figure 7. Critical behaviour of the parameters C'' and D'' versus composition.

4. Discussion

As follows from the previous section, the SE model of the VRH conductivity provides a consistent description of the local activation energy of LCMO over the whole temperature interval, including both the stable and the critical regimes. This model takes into account the generation of the Coulomb gap around the Fermi level. On one hand, it has been shown above that in LCMO the width of the gap practically coincides with the energy of the Coulomb repulsion between the localized carriers. On the other hand, the existence of a gap with the width of 0.215 eV in the DOS was found recently in variable-temperature scanning tunnelling microscopy/spectroscopy studies of LCMO with $x = 0.2$ [32]. This value is quite close to that found in our work (table 1). The critical exponent $\nu \approx 1$ is the same as that determining the divergence of the correlation length at the MIT in doped semiconductors [31]. The value of ξ' found above in the stable regime (table 1) is also very close to the carrier localization radius $\xi \approx 5$ Å estimated from Gaussian fluctuations in the magneto-thermopower of $La_{0.6}Y_{0.1}Ca_{0.3}MnO_3$ [33]. On the other hand, the value of ξ' satisfies the condition $\xi' \leqslant r_p$ where $r_p = (1/2)(\pi/6N_s)^{1/3} \approx 5.4$ Å is the limiting size of a small lattice polaron [24].

As mentioned in the introduction, only the Mott-VRH regime has been considered to interpret the conductivity of different CMR materials [18–23]. In this way, e.g. for $La_{1.5}Sr_{0.5}MnRhO_6$, $\xi \approx 2$ Å was obtained, assuming the DOS at the Fermi level to be $g(\mu) \approx 10^{20}$ eV^{-1} cm^{-3} [23]. It is easy to show that similar values of the correlation length would be found for our LCMO samples if we supposed Mott-VRH conductivity and considered only figure 3(b). In fact, in the Mott regime we have $T_0 = 21/[k\xi^3 g(\mu)]$ [25] and the linear

fits of the plots in figure 3(b) below T_C yield $T_0 = 7.6 \times 10^7$, 5.7×10^7 and 6.0×10^7 K, giving $\xi' = 2.4$, 2.8 and 2.6 Å for the samples #1, #2 and #3, respectively (here we use the values of $g(\mu) = g_0$ found above). However, these values of ξ' are contradictory, because for $T < T_C$ they lead to the average hopping length, $R_h = (3/8)\xi'(T_0/T)^{1/4} \approx 8$–10 Å which is smaller than the average distance between the hopping sites $R_s \approx 16$–17 Å. Similar contradictions were found in the analysis of the VRH conductivity with the Mott law for the insulating phase of $La_{0.7}Sr_{0.3}MnO_3$, giving $\xi = 1.3$ Å [18], and even more drastic ones yielding completely unphysical values of ξ for $Pr_{0.7}Pb_{0.3}MnO_3$ ($\xi = 0.2$ Å [18]), $Sm_{0.7}Sr_{0.3}MnO_3$ ($\xi = 0.26$ Å [19] and 0.29 Å [20]) and $La_{0.7}Ca_{0.3}MnO_3$ ($\xi = 0.56$ Å [19]). Due to these contradictions in [18] the 'magnetic localization' mechanism has been proposed and used to interpret the data in references [18–20], yielding a better value of $\xi = 4.5$ Å for $La_{0.7}Sr_{0.3}MnO_3$ but still too small a value of $\xi = 0.8$ Å for $Pr_{0.7}Pb_{0.3}MnO_3$ [18]. On the other hand, in [19] it was mentioned that for the $Sm_{0.7}Sr_{0.3}MnO_3$ sample the SE-VRH mechanism with $p = 1/2$ also gives a satisfactory fit to the temperature dependence of the resistivity. However, the SE model was applied to interpret the resistivity data neither in this nor in the other papers cited earlier.

Investigations of infrared optical properties of $La_{0.7}Ca_{0.3}MnO_3$ thin films [34] at 300 K have yielded the value of the high-frequency dielectric permeability $\kappa_\infty \approx 9$ which is greater than $\kappa' \approx 3.6$ found above. Taking into account that the static permeability κ_0 exceeds κ_∞, the meaning of the parameter κ used in this work should be refined. In equations (4) κ appears as a result of taking into account the energy $U \approx e^2/\kappa R_s$ of the Coulomb interaction between the localized charge carriers. For $R_s \gg a$ (the lattice parameter) the continuum approximation is valid and $\kappa = \kappa_0$, while for $R_s < a$ the value of $\kappa \approx 1$. However, we have $a = 7.8$ Å and $R_s \approx 16$–17 Å which represents a crossover between these two limits. In such a case it is natural to expect that $1 < \kappa < \kappa_0$. Hence, κ does not represent the true static dielectric permeability but is only an effective parameter, which describes the Coulomb interaction between the localized charge carriers when the continuum approximation does not work.

The observed behaviour of the local activation energy with reduction of temperature is consistent with the following interpretation. In the stable regime our resistivity data can be interpreted in terms of hopping of small lattice polarons in the PM phase of LCMO. As T tends to T_C', entering the critical region of the VRH conductivity, a small fraction of the lattice polarons act as centres for generation of magnetic polarons. In the critical regime the radius of the magnetic polarons exhibits a critically rapid growth. The value of T_C' corresponds to the divergence of the correlation length, while the PM–FM transition may occur even at a finite value of the polaronic radius. In fact, if the PM–FM transition were percolative in nature, then it would be governed by generation of an infinite cluster of overlapping magnetic polarons. The volume fraction of the polarons can be written as

$$\theta(T) = (4\pi/3)\eta n_h(\xi_2')^3 = (4\pi/3)\zeta n_h(\xi_1')^3\,(1 - T_C'/T)^{-3\nu}.$$

The generation of the infinite cluster takes place when the volume fraction of the polarons reaches the critical value $\theta_c = 0.29$ [25]. At $\theta(T_C) = \theta_c$ we obtain

$$\frac{T_C'}{T_C} = 1 - \left[\frac{4\pi\zeta' n_h(\xi_1')^3}{3\theta_c}\right]^{1/3\nu} \tag{11}$$

and $T_C'/T_C = 0.955 \pm 0.004$, in excellent agreement with the observed value 0.95 ± 0.02 (see section 3). This confirms the percolative character of the PM–FM transition in our LCMO samples.

The divergence of the correlation length suggests that we are dealing with a MIT. However, in sample #3 which has the highest x the metallic conductivity with zero activation energy is observed only within a narrow temperature interval (T_m, T_m^*) while in samples #1 and #2 it

is not observed at all. The reason is a decomposition of the metallic FM phase caused by a critically rapid decrease of the polaron radius, when the correlation length restores a finite value. This occurs below T_C''. For sample #3, $T_C'' < T_C'$; therefore there exists a small temperature window of the FM metallic state. For sample #2, we have $T_C'' \approx T_C'$, while for sample #1, T_C'' even exceeds T_C' and coincides with T_C, which indicates a transition into a mixed, or partially disordered FM phase with a large but always finite correlation length. This agrees well with the susceptibility data shown in figure 2. We see that the onset of the magnetic irreversibility or deviation of $\chi_{ZFC}(T)$ from $\chi_{FC}(T)$ typical for a frustrated SG or mixed (FM + SG) state practically coincides with the steep increase of both susceptibilities identified as the FM–PM transition at T_C. Because $\zeta'' \gg \zeta'$, after destruction of the FM or the mixed state the number of magnetic polarons is not conserved. This suggests the existence of an intermediate strongly (or even completely) polarized state, which splits into finite-size magnetic polarons below T_C'' generating a new phase, different from that above T_C'.

At a temperature T_G between ~90 and 70 K (decreasing when x is increased) which is well below T_C'', the onset of the frequency dependence of the ac susceptibility is observed [30]. The frequency dependence of T_G is described by a critical slowing-down law characterized by a minimum relaxation time $\sim 10^{-12}$ s, which is typical for a spin-flip frequency of atomic-size spins [30]. Therefore, in the interval $T < T_G$ the magnetic polarons should have a small radius, as in the PM phase, or even vanish. This is valid provided that the value of x is sufficiently small. When x is increased, the correlation length below T_C'' increases according to the scaling law (see the end of section 3). As $x \to x_t$, the divergence of ξ'' indicates vanishing of the insulating state at $T < T_C$ above $x_t \approx 0.175$. Experimentally the metallic phase is observed in LCMO at $T < T_C$ starting from $x = 0.2$ [7]. Therefore, investigations between $x \approx 0.15$ and 0.2 would be interesting, to see how the metallic phase gradually sets in.

The scenario described above is similar to that observed recently in LCMO with $x \approx 0.3$ by means of muon spin-relaxation and neutron spin-echo measurements [35] where the existence of two spatially separated regions in close proximity possessing very different Mn-ion spin dynamics was found. One of the regions corresponds to an extended cluster, displaying critical slowing down near T_C and increasing volume fraction below T_C. The second region possesses more slowly fluctuating spins and decreasing volume fraction below T_C. This behaviour was explained as reflecting formation and accretion of magnetoelastic polarons, which have an influence on the FM transition.

5. Conclusions

The resistivity of LCMO with $0 \leqslant x \leqslant 0.15$ and $c = 0.18$–0.22 is shown to have an activated character both above and below T_C. The temperature dependence of the local activation energy in the PM phase manifests the VRH conductivity over the states of the Coulomb gap. The effective dielectric permeability, the value of the gap and the correlation length of the charge carriers are determined. Values of ξ and Δ very close to our results were obtained independently in [32, 33]. The value of $\xi' \leqslant r_p$ is consistent with hopping of small lattice polarons. With decreasing T two successive transitions are observed, corresponding to temperatures T_C' and T_C'' associated with the divergence of the correlation length. They can be interpreted in terms of critical increase (as T approaches T_C' from higher temperatures) and decrease (when T shifts from T_C'' towards lower temperatures) of the radius of the magnetic polarons, which can be generated by a small fraction of the lattice polarons as $T \to T_C$. The difference between T_C and T_C' gives evidence for percolative character of the FM–PM transition.

References

[1] Wollan E O and Koehler W C 1955 *Phys. Rev.* **100** 545
[2] Mahendrian R, Tiwary S K, Raychaudhuri A K, Ramakrishnan T V, Mahesh R, Rangavittal N and Rao C N R 1996 *Phys. Rev.* B **53** 3348
[3] Töpfer J and Goodenough J B J 1997 *Solid State Chem.* **130** 117
[4] de Gennes P-G 1960 *Phys. Rev.* **118** 141
[5] Schiffer P, Ramirez A P, Bao W and Cheong S-W 1995 *Phys. Rev. Lett.* **75** 3336
[6] von Helmolt R, Wecker J, Holzapfel B, Schulz L and Samwer K 1993 *Phys. Rev. Lett.* **71** 2331
[7] Ramirez A P 1997 *J. Phys.: Condens. Matter* **9** 8171
[8] Alexandrov A S and Bratkovsky A M 1999 *Phys. Rev. Lett.* **82** 141
[9] Varma C M 1996 *Phys. Rev.* B **54** 7328
[10] Meneghini C, Castellano C, Kumar A, Ray S, Sarma D D and Mobilio S 1999 *Phys. Status Solidi* b **215** 647
[11] Hennion M, Moussa F, Biotteau G, Rodriguez-Carvajal J, Piusard L and Revcolevschi A 1998 *Phys. Rev. Lett.* **81** 1957
[12] Mellergård A, McGreevy R L and Eriksson S G 2000 *J. Phys.: Condens. Matter* **12** 4975
[13] Jaime M, Salamon M B, Rubinstein M, Treece R E, Horwitz J S and Chrisei D B 1996 *Phys. Rev.* B **54** 11 914
[14] Jaime M, Hardner H T, Salamon M B, Rubinstein M, Dorsey P and Emin D 1997 *Phys. Rev. Lett.* **78** 951
[15] Palstra T T, Ramirez A P, Cheong S-W, Zegarski B R, Schiffer P and Zaanen J 1997 *Phys. Rev.* B **56** 5104
[16] Cao X M, Fang J, Wang Z H and Li K B 1999 *J. Appl. Phys.* **75** 3372
[17] Zhao G, Keller H and Prellier W 2000 *J. Phys.: Condens. Matter* **12** L361
[18] Viret M, Ranno L and Coey J M D 1997 *Phys. Rev.* B **55** 8067
[19] Viret M, Ranno L and Coey J M D 1997 *J. Appl. Phys.* **81** 4964
[20] Thomas R M, Ranno L and Coey J M D 1997 *J. Appl. Phys.* **81** 5763
[21] Liu J-M, Huang Q, Li J, Ong C K, Wu Z C, Liu Z G and Du Y W 2000 *Phys. Rev.* B **62** 8976
[22] Coldea A I, Marshall I M, Blundell S J, Singleton J, Noailles L D, Battle P D and Rosseinsky J 2000 *Phys. Rev.* B **62** R6077
[23] De Tereza J M, Ibarra M R, Blasko J, Garcia J, Marquina C, Algarabel P A, Arnold Z, Kamenev K, Ritter C and von Helmolt R 1996 *Phys. Rev.* B **54** 1187
[24] Mott N F and Davies E A 1979 *Electron Processes in Non-Crystalline Materials* (Oxford: Clarendon)
Mott N F 1990 *Metal–Insulator Transitions* (London: Taylor and Francis)
[25] Shklovskii B I and Efros A L 1984 *Electronic Properties of Doped Semiconductors* (Berlin: Springer)
[26] Laiho R, Lisunov K G, Lähderanta E, Petrenko P, Stamov V N and Zakhvalinskii V S 2000 *J. Magn. Magn. Mater.* **213** 271
[27] Miller R C, Heikes R R and Mazelsky R 1961 *J. Appl. Phys.* **32** 2202
[28] Hashimoto T, Ishizawa N, Mizutani N and Kato M 1988 *J. Mater. Sci.* **23** 1102
[29] Laiho R, Lisunov K G, Lähderanta E, Petrenko P, Salminen J, Stamov V N and Zakhvalinskii V S 2000 *J. Phys.: Condens. Matter* **12** 5751
[30] Laiho R, Lisunov K G, Lähderanta E, Salminen J and Zakhvalinskii V S 2000 *Phys. Rev.* B to be published
[31] Castner T G 1991 *Hopping Transport in Solids* ed M Pollak and B Shklovskii (Amsterdam: Elsevier)
[32] Biswas A, Elizabeth S, Raychaudhuri A K and Bhat H L 1999 *Phys. Rev.* B **59** 5368
[33] Sergeenkov S, Bougrine H, Ausloos M and Gilabert A 1999 *Phys. Rev.* B **60** 12 322
[34] Boris A V, Kovaleva N N, Bazhenov A V, Samoilov A V, Yeh N-C and Vasquez R P 1997 *J. Appl. Phys.* **81** 5756
[35] Heffner R H, Sonier J E, MacLaughlin D E, Nieuwenhuys G J, Ehlers G, Mezei F, Cheong S-W, Gardner J S and Röder H 2000 *Phys. Rev. Lett.* **85** 3285